CHAPTER 4

PARAMETRIC STUDY THROUGH NUMERICAL MODELLING

4.1. Introduction

FLAC (Fast Lagrangian Analysis of Continua) 2D, Version 7.0 software (FLAC 2011) was used in the parametric study for measuring the sensitivity of the major parameters governing the stability of the dump slope structures. It is a finite difference method based software which uses a strength reduction technique to calculate the safety factor of the dump slope structure.

4.2. Effect of the Total Dump Height

In the present study, dump height was varied from 90 – 420 m, and the base value of density, bench height, slope angle, bench width, cohesion, and friction angle were adopted from Table 3.2 while analyzing the behaviour of total dump height on the stability of dump slope structure. The parametric study results indicated that the FoS of the dump slope structure reduced from 1.56 to 1.02 for an increase in the total dump height from 90 to 420 m in stages of 30m (Figure 4.1). A nonlinear inversely proportional relationship was observed between total dump height and FoS. The decrement rate of FoS was approximately the same upon increasing the height from 90 to 420 m. However, a significant drop of FoS was seen between 330 to 360 m dump height, and then again, it gradually decreased from 360 to 420 m. The XDIS and SSI possessed a nonlinear directly proportional relationship with the total dump height of the slope structure, as presented in Figures 4.2 and 4.3, respectively. The XDIS and SSI also suggested deviation in the curve trend between 300 to 360 m dump height. Figure 4.2 depicts that the maximum horizontal deformation increased from 1 to 35 mm with the increase in total dump height from 90 to 420 m. The maximum value of the shear strain increment rose from 0.0007 to

0.01 for this increase in the total dump height. The variation in the maximum horizontal displacement and shear strain increment nearly followed a similar trend from 90 to 300 m.

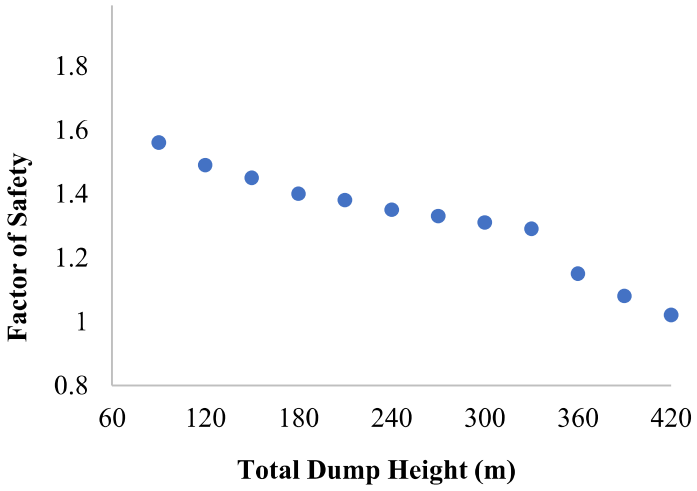

Fig. 4.1 Total Dump Height versus Factor of Safety

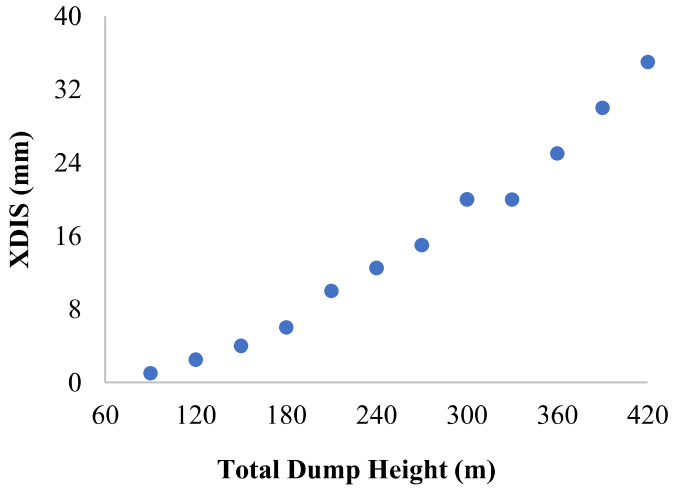

Fig. 4.2 Total Dump Height versus Max Horizontal Displacement

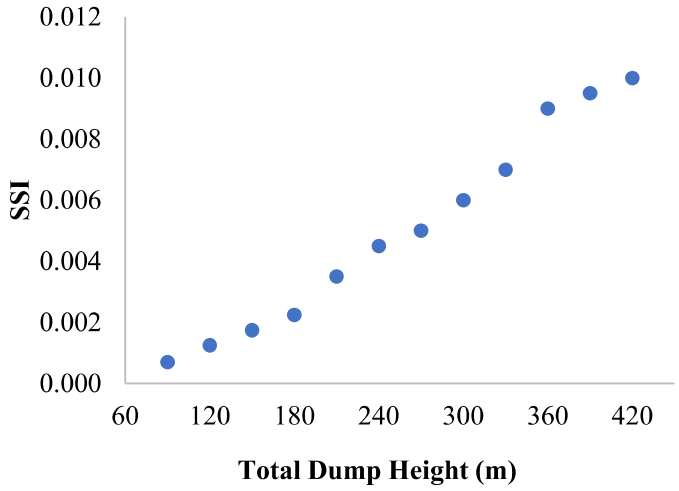

Fig. 4.3 Total Dump Height versus Max Shear Strain Increment

Figure 4.4 shows the increment of the vulnerable zone in black with the increase in the total dump height. It was observed that the vulnerable zone occurred beyond 180 m dump height, and it initiated from the middle benches, as illustrated in Figure 4.4 (a). The growth vulnerable zone increased gradually from 270 to 300 m (Figures 4.4 (a) - (b)), but it increased abruptly from 300 to 360 m (Figures 4.4 (c) - (d)) and again increased gradually from 360 to 420 m dump height (Figures 4.4 (e) - (f)). Hence, the abnormal trend was noticed in the FoS, XDIS, and SSI curves between 300 to 360 m, as depicted in Figures 4.1 – 4.3. The instability zone was concentrated near the toe of the middle benches, and it rose from the toe to the crest towards the upper side benches with the increase in dump height. The significant area was influenced beyond 300 m. It was seen that the bottom-most two benches experienced low displacement compared to the remaining benches and were less susceptible to failure.

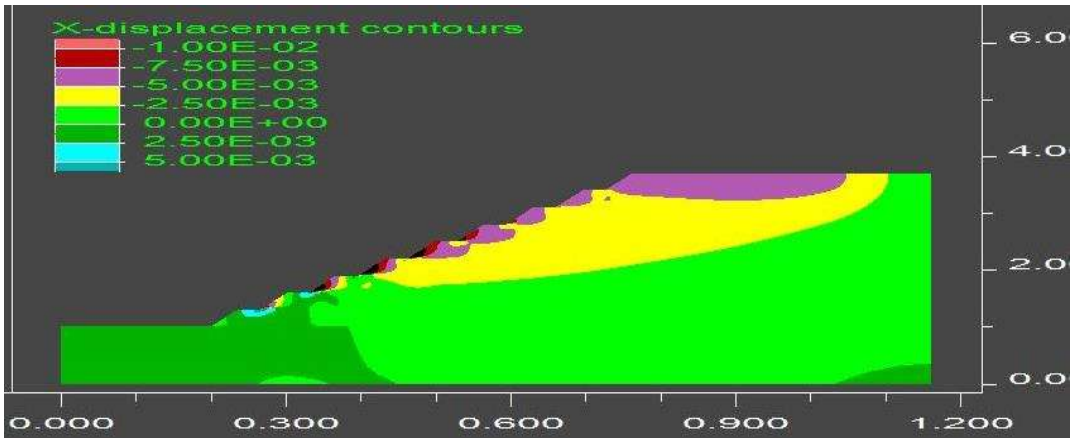

(a) 270 m

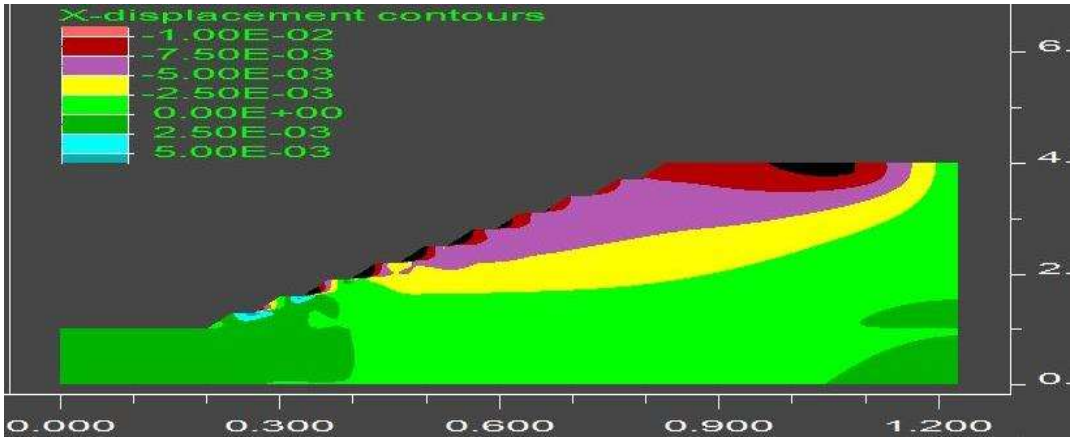

(b) 300 m

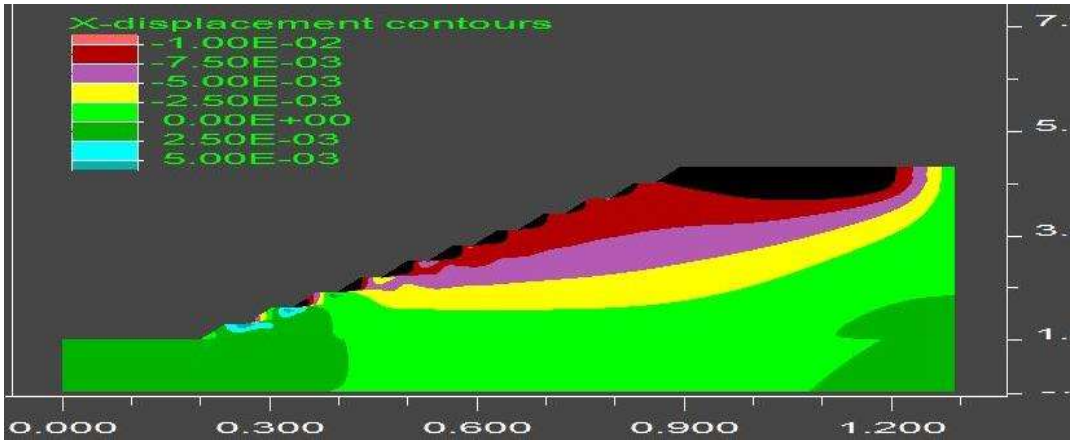

(c) 330 m

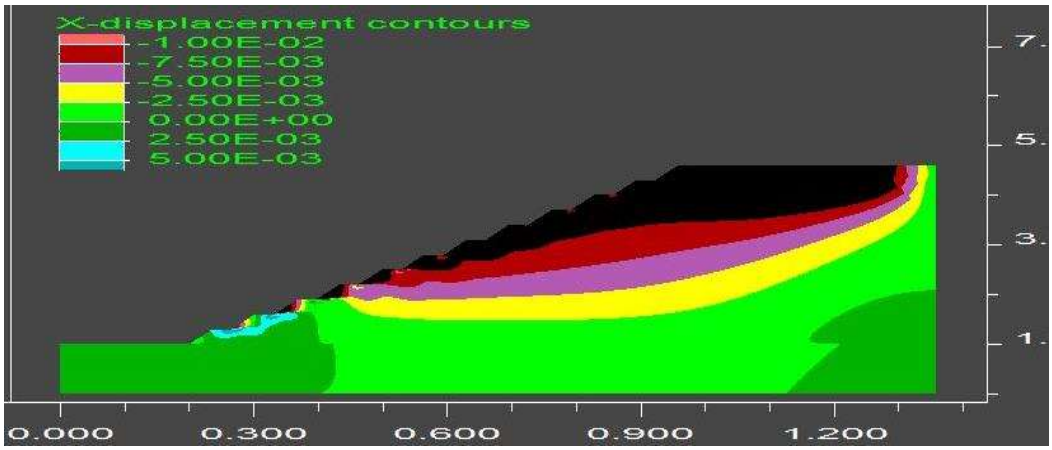

(d) 360 m

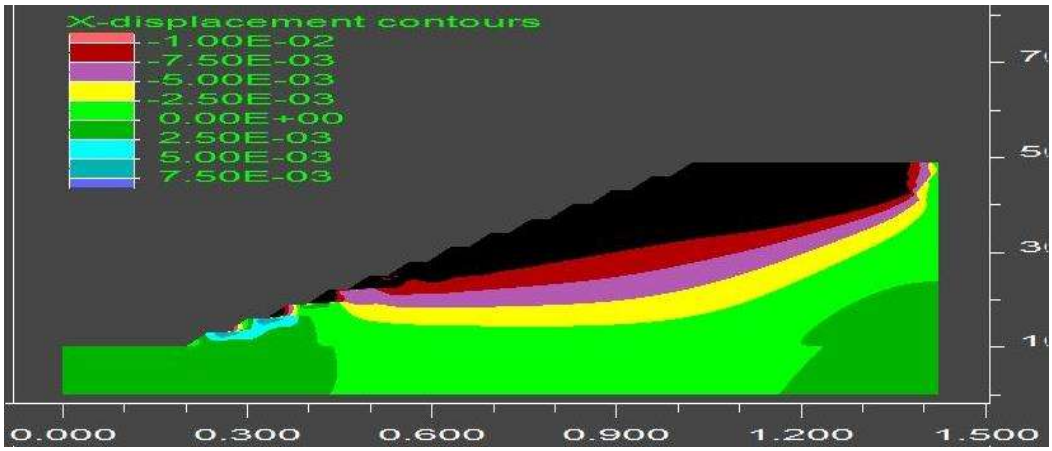

(e) 390 m

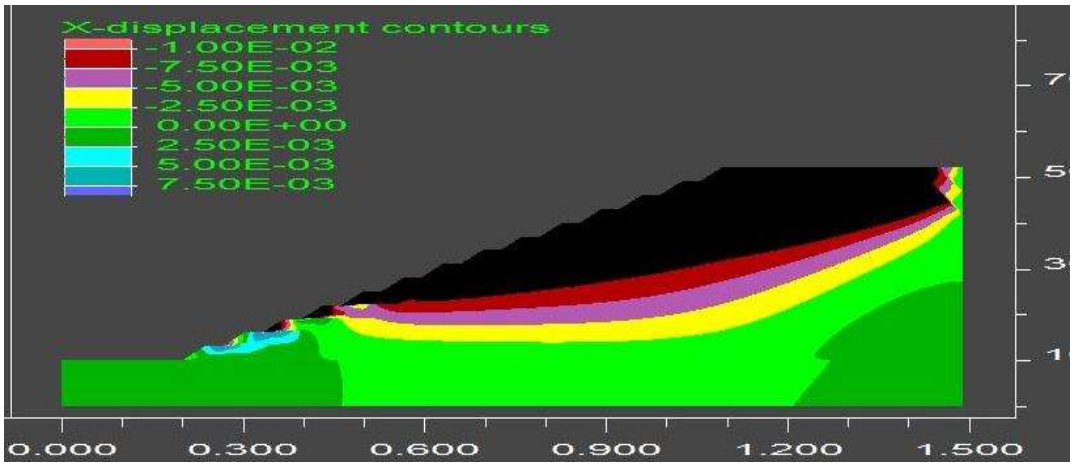

(f) 420 m

Fig. 4.4 Zone of influence corresponding to dump height (1 unit of X = 1000 m & Y axis = 100 m)

4.3. Effect of the Bench Height

The sensitivity analysis of the bench height was performed by varying it from 10 to 50 m in the increment of 10 m in each step with the base value of the remaining parameters. Figure 4.5 depicts that the safety factor of the dump slope structure decreased from 2.58 to 1.17 while the bench height increased for the considered range. The FoS was reduced by approximately 34 % by increasing the bench height from 10 to 20 m, and an overall drop of about 55% was obtained in FoS by moving from 10 to 50 m. The increment in horizontal displacement was low from 10 to 20 m bench height but increased significantly from 20 to 50 m, as shown in Figure 4.6. The XDIS was magnified from 1.25 to 20 mm for this increase in the bench height. The SSI followed a different trend from the XDIS and possessed a logarithmic nature. The SSI enhanced from 0.0002 to 0.003 for the increase in bench height from 10 to 50 m (Figure 4.7). It became constant after 40 m bench height.

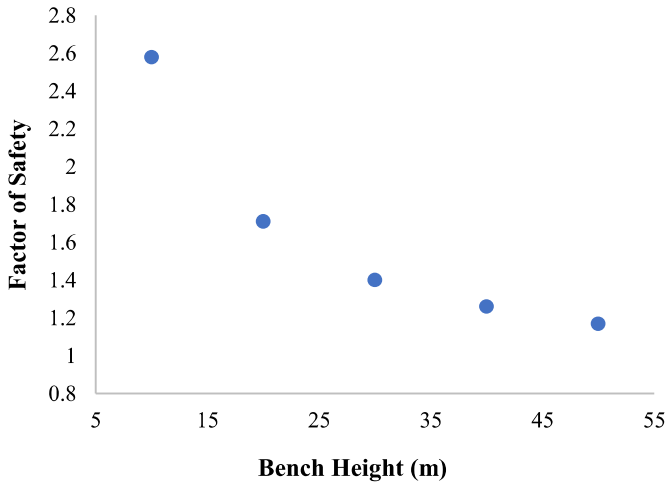

Fig. 4.5 Bench Height versus Factor of Safety

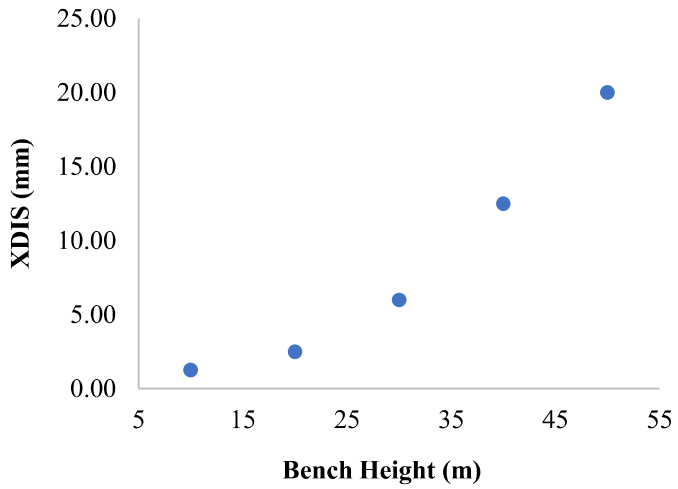

Fig. 4.6 Bench Height versus Max Horizontal Displacement

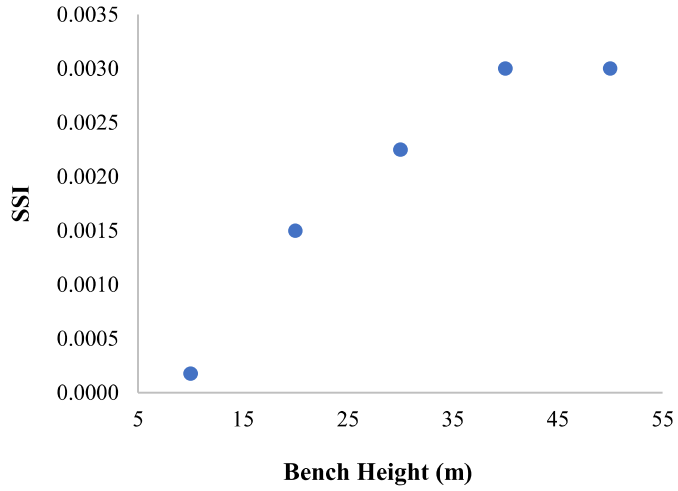

Fig. 4.7 Bench Height versus Max Shear Strain Increment

The progression of the vulnerable zone due to an increase in the bench height is illustrated in Figure 4.8. The XDIS was insignificant until 30 m bench height. The vulnerable zone was initiated when the bench height was greater than 30 m. The vulnerable zone was present at the toe of the second bottom-most bench (Figure 4.8 (a)), and it rose and also influenced the bottom-most bench after increasing the bench height by 10 m (Figure 4.8

(b)). In this case, the vulnerable zone again initiated from the 2nd bottom most bench of the dump slope structure, but it progressed downward with the increase of bench height.

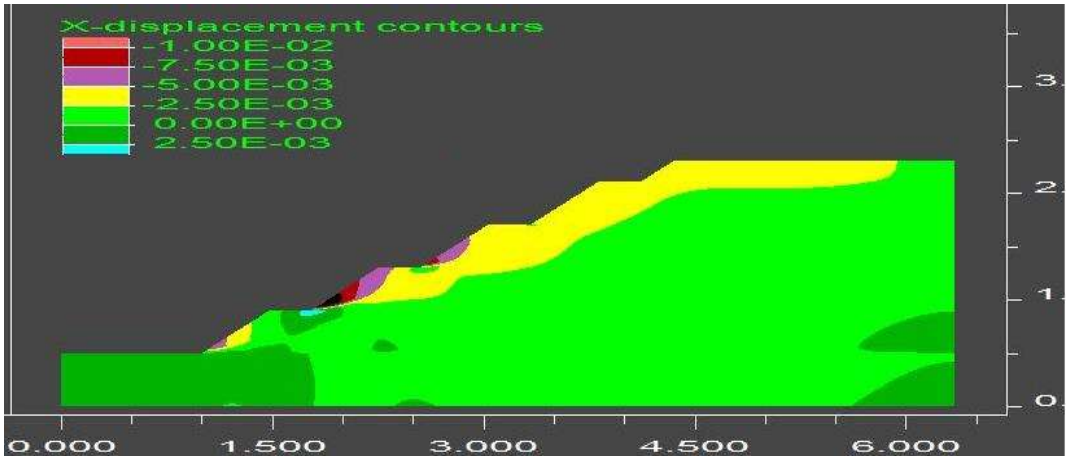

(a) 40 m

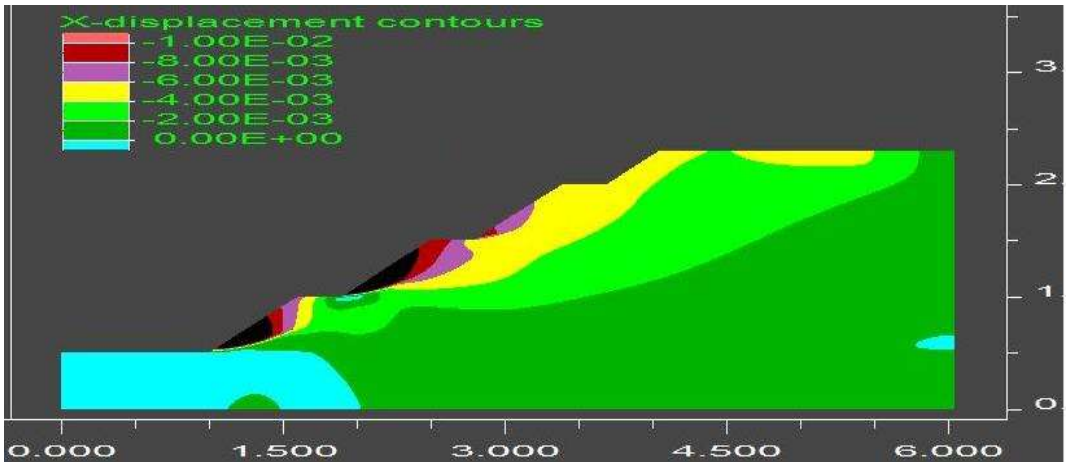

(b) 50 m

Fig. 4.8 Zone of influence corresponding to bench height (1 unit of X & Y axis = 100 m)

4.4. Effect of the Bench Slope Angle

The bench slope angle of the OB dump slope varied from 30 to 50º in increments of 5º to evaluate its effect on the structure stability. Figure 4.9 illustrates that the bench slope angle had a nonlinear inverse relationship with the stability of the dump slope structure. The study described that the FoS of the dump slope reduced from 1.72 to 1.20 for an

increased bench slope angle. The maximum horizontal displacement extended exponentially as the bench slope angle increased from 30 to 50º (Figure 4.10). The XDIS was magnified from 2 to 15 mm for the adopted range. The rate of increment was amplified after each succession. The shear strain increment also increased from 0.0012 to 0.005 as the bench slope angle increased (Figure 4.11). The SSI was constant for 35º and 40º, but it increased with a further increase in the bench slope angle.

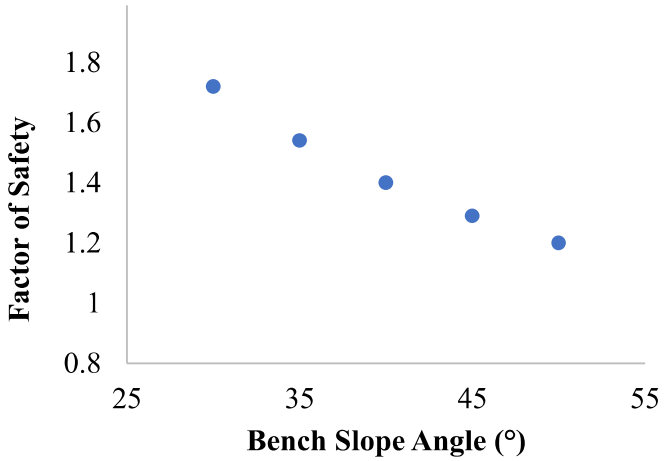

Fig. 4.9 Bench Slope Angle versus Factor of Safety

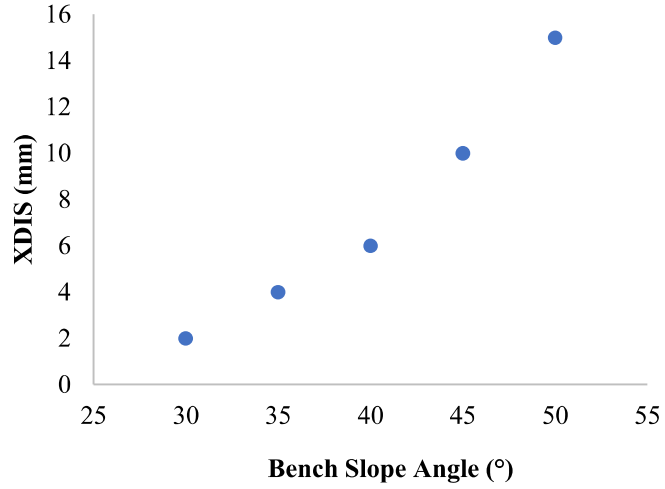

Fig. 4.10 Bench Slope Angle versus Max Horizontal Displacement

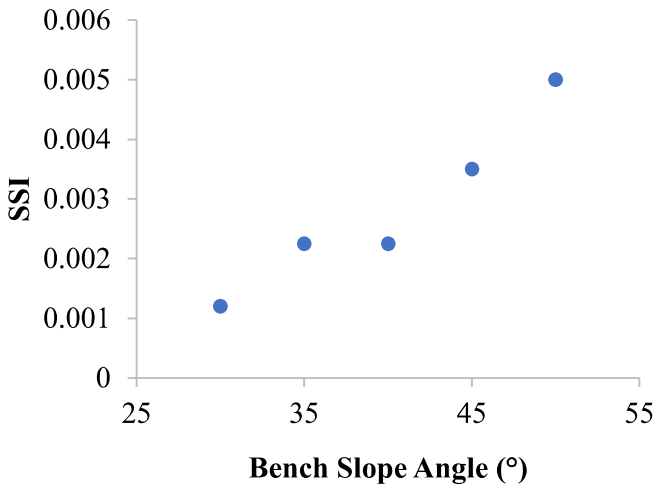

Fig. 4.11 Bench Slope Angle versus Max Shear Strain Increment

The vulnerable zone originated from the 2nd bottommost and middle bench of the dump slope structure while increasing the bench slope angle above 40° (Figure 4.12 (a)). It was present at the toe of the benches, and it became intense by increasing the bench slope angle to 50° (Figure 4.12 (b)). The XDIS enhanced to the adjacent lower and upper bench while increasing the slope angle. The topmost two benches also experienced displacement but were not high. The XDIS was small on maintaining the bench slope angle below 45°.

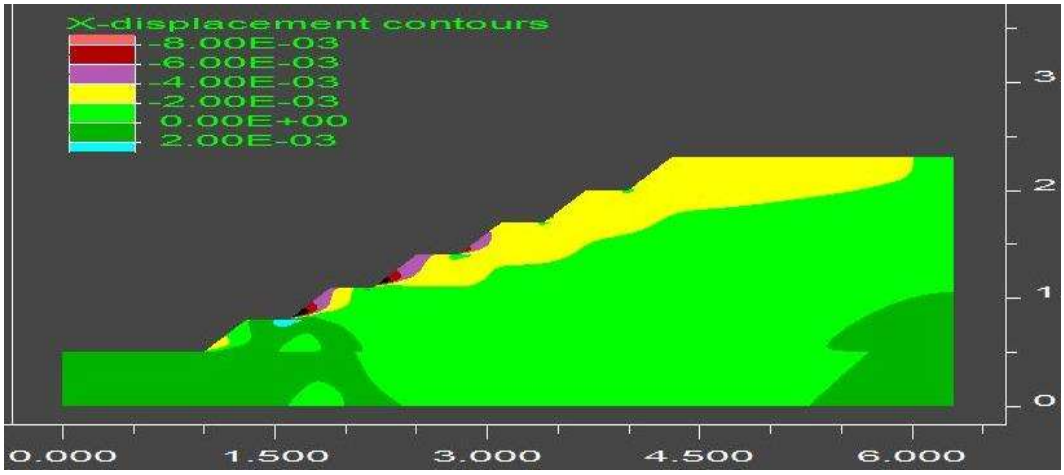

(a) 45°

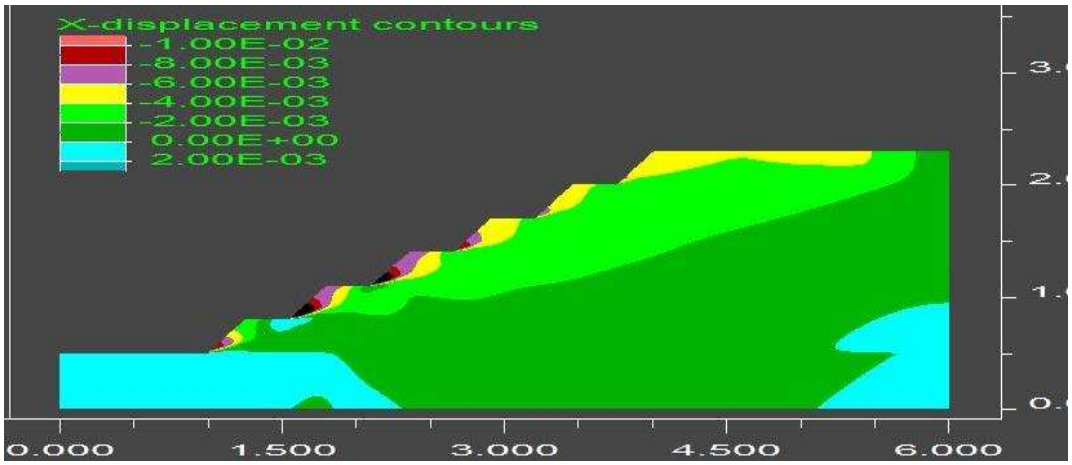

(b) 50°

Fig. 4.12 Zone of influence corresponding to bench slope angle (1 unit of X & Y axis = 100 m)

4.5. Effect of the Bench Width

The impact of bench width was examined by varying it from 5 to 40 m in stages of 5 m. The increment of the bench width improved the stability of the dump slope linearly (Figure 4.13). The FoS increased from 0.9 to 1.58 by increasing the bench width from 5 to 40 m. The increment rate was constant throughout the considered range. The dump slope structure was unstable or near failure when the bench width was less than or equal to 10 m. The maximum horizontal displacement and shear strain increment were inversely proportional to the bench width, as illustrated in Figures 4.14 and 4.15, respectively. The max XDIS and SSI magnitude was very high at a bench width of 5 m compared to 10 – 40 m. Therefore, the max XDIS and SSI range zoomed in for more insight, as represented in Figures 4.14 (b) and 4.15 (b), respectively. The max XDIS dropped from 12500 to 5 mm with increased bench width (Figure 4.14). The XDIS reduced drastically by 312.5 times when the bench width moved from 5 to 10 m (Figure 4.14 (a)). The XDIS again reduced significantly about 2.67 times as bench width increased from 10 to 15 m (Figure 4.14 (b)). The SSI decreased from 0.6 to 0.002 with the increase in the bench width

(Figure 4.15). The SSI at 5 m bench width was 100 times higher than the 10 m bench width (Figure 4.15 (a)). The reduction in SSI was also very high for an increase in the bench width from 10 to 15 m (Figure 4.15 (b)). The SSI was reduced twice by increasing the bench width from 10 to 15 m. The SSI attained a magnitude of 0.0025 from 20 to 35 m bench width, and a small drop was noted at 40 m.

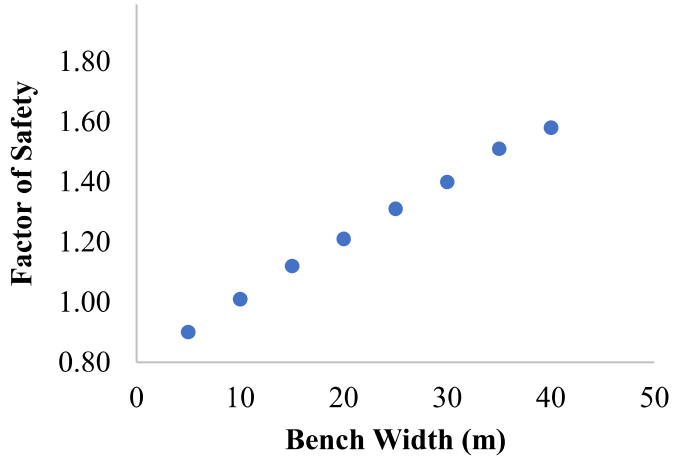

Fig. 4.13 Bench Width versus Factor of Safety

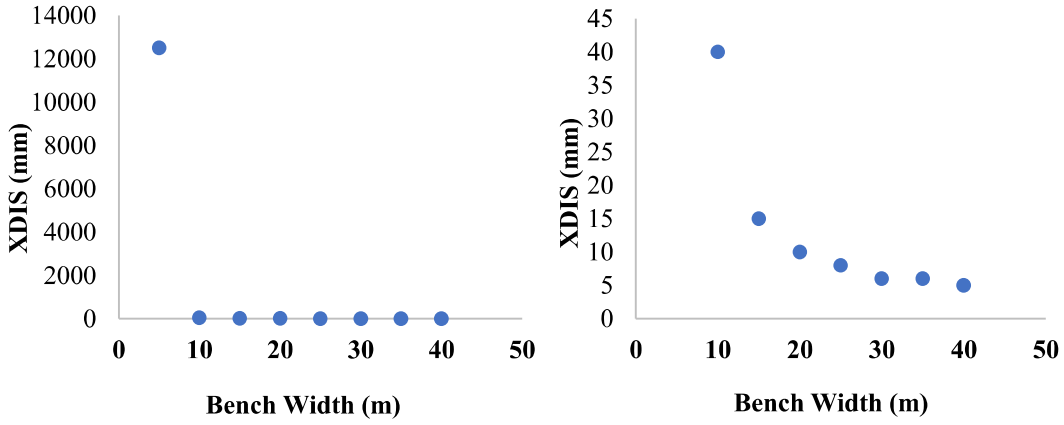

(a) Bench Width 5-40 m (b) Bench Width 10-40 m

Fig. 4.14 Bench Width versus Max Horizontal Displacement

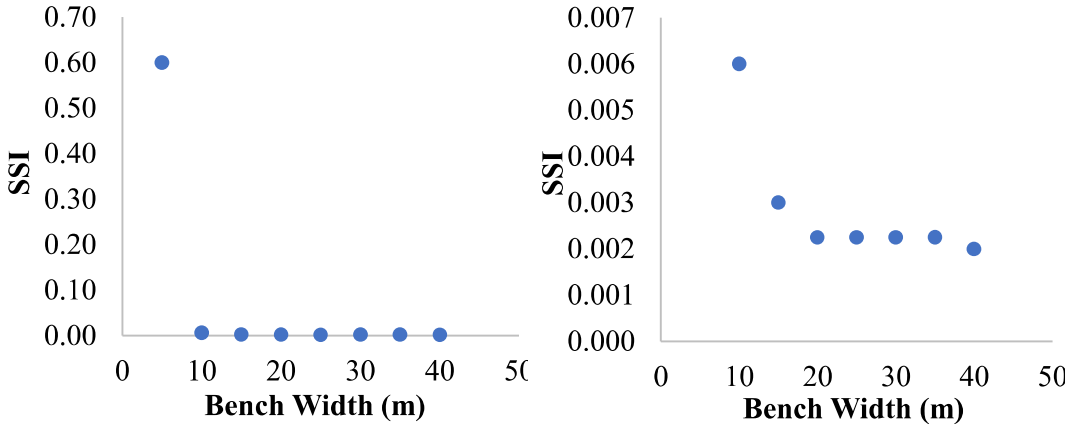

(a) Bench Width 5-40 m (b) Bench Width 10-40 m

Fig. 4.15 Bench Width versus Max Shear Strain Increment

The horizontal displacement was small when the bench width was greater than 25 m. The vulnerable zone was induced when the bench width was less than 25 m. Figure 4.16 (a) shows the vulnerable zone initiated from the 2nd and 3rd bottom most benches and located at the toe. It moved downward with increased influencing area by reducing the bench width from 20 to 15 m (Figure 4.16 (b)). At 10 m bench width, all benches were in a vulnerable zone except the top most bench, as presented in Figure 4.16 (c).

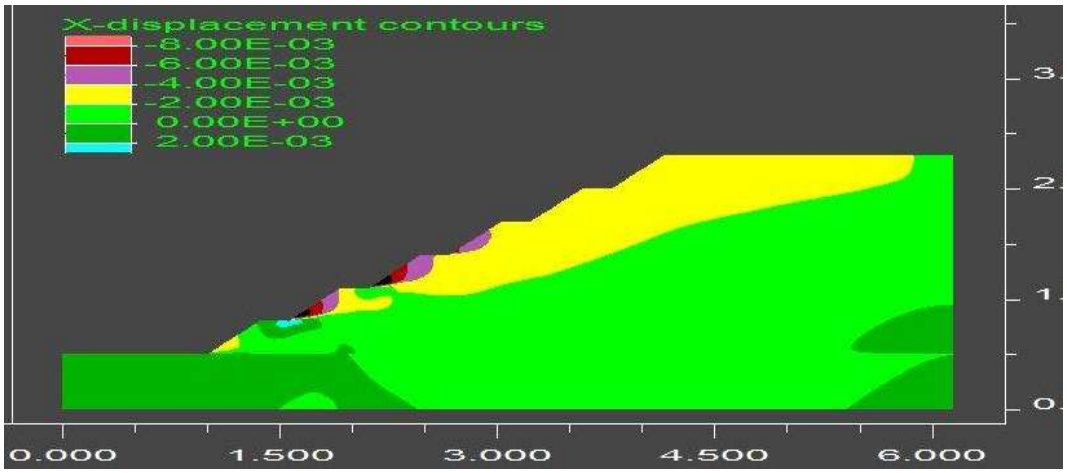

(a) 20 m

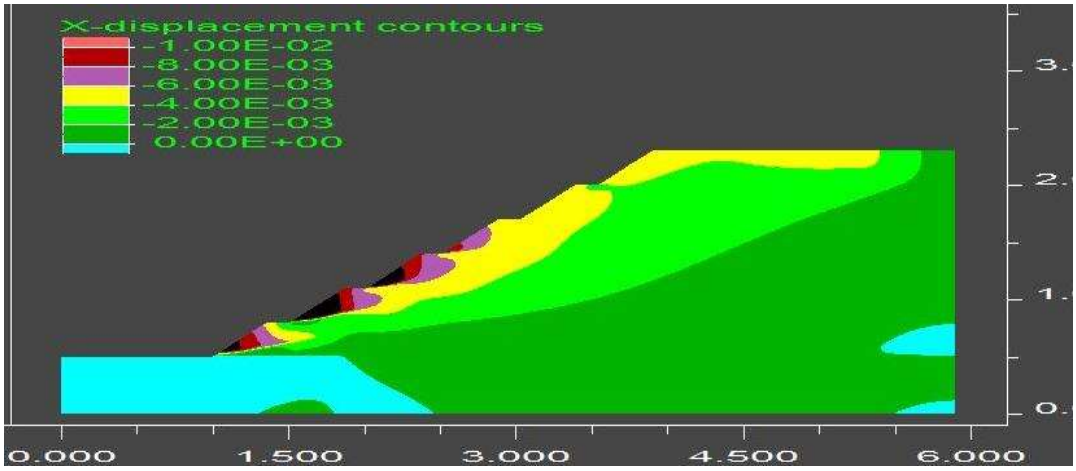

(b) 15 m

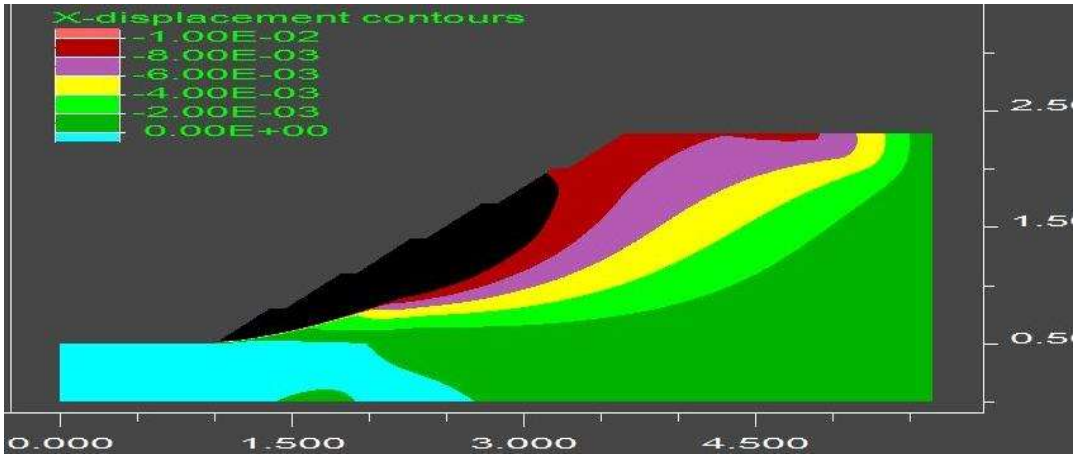

(c) 10 m

Fig. 4.16 Zone of influence corresponding to bench width (1 unit of X & Y axis = 100 m)

4.6. Effect of the Cohesion

The safety factor of the dump slope structure enhanced from 0.92 to 1.57 with the increase in the cohesive strength of the dump material from 0.01 to 0.09 MPa in stages of 0.02 MPa (Figure 4.17). The cohesion of the OB dump slope was directly proportional to the stability, and the trend of the FoS curve followed the logarithmic nature. The increment rate of FoS was high while moving from 0.01 to 0.03 MPa compared to the rest of the cohesion value. The XDIS and SSI were inversely proportional to the cohesion (Figures 4.18 and 4.19). There was a drastic change in the magnitude of XDIS and SSI as

increasing cohesion from 0.01 to 0.03 MPa. The XDIS and SSI decrement rate was significant between 0.01 to 0.03 MPa against the remaining points. A magnified view of XDIS and SSI from 0.03 to 0.09 MPa was illustrated in Figures 4.18 (b) and 4.19 (b), respectively. The XDIS diminished from 125000 to 10 mm for enhancing cohesion from 0.01 to 0.03 MPa and from 10 to 3 mm between the cohesion of 0.03 to 0.09 MPa. The SSI dropped from 17.5 to 0.003 by increasing cohesion from 0.01 to 0.03 MPa and from 0.003 to 0.0015 between 0.03 to 0.09 MPa cohesion.

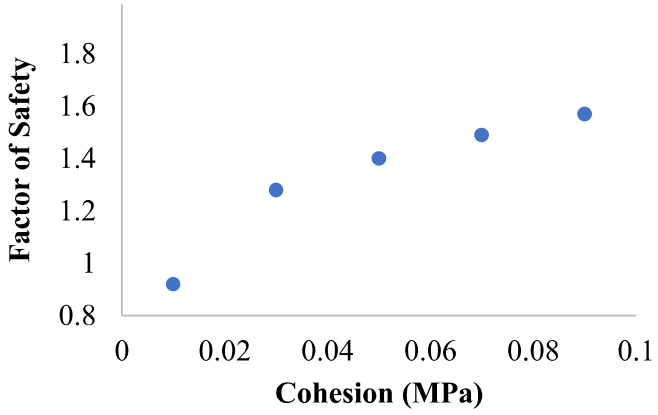

Fig. 4.17 Cohesion versus Factor of Safety

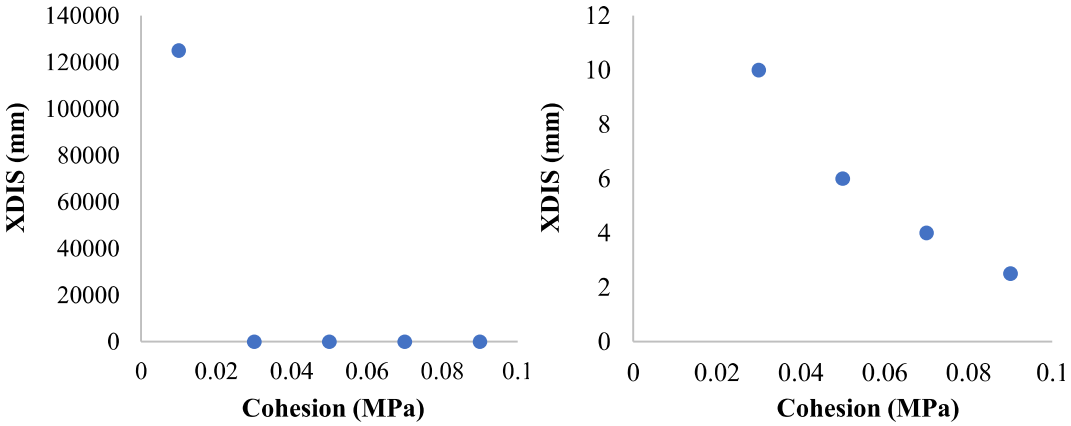

(a) Cohesion 0.01-0.09 MPa (b) Cohesion 0.03-0.09 MPa

Fig. 4.18 Cohesion versus Max Horizontal Displacement

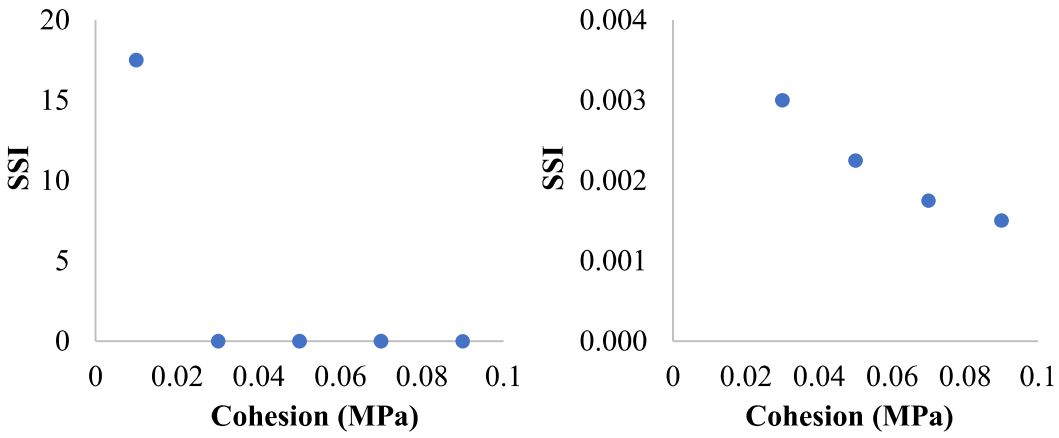

(a) Cohesion 0.01-0.09 MPa (b) Cohesion 0.03-0.09 MPa

Fig. 4.19 Cohesion versus Max Shear Strain Increment

The vulnerable zone was initiated when OB material possessed cohesion of 0.02 MPa or less, as depicted in Figure 4.20. The toe of the middle benches experienced high horizontal displacement compared to the top and bottom-most benches. The vulnerable zone moved in upward and downward directions from the middle benches while reducing cohesion. The vulnerable zone did not exist when cohesion was greater than 0.02 MPa.

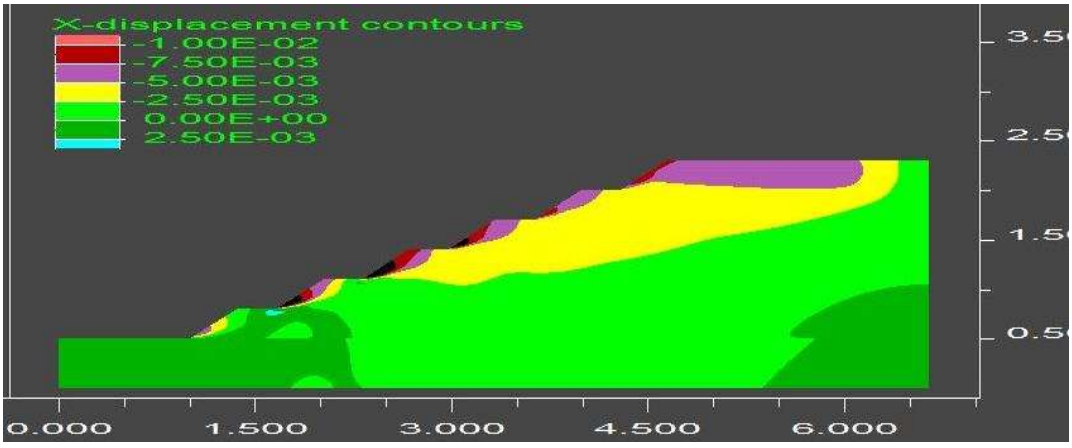

Fig. 4.20 Zone of influence corresponding to cohesion 0.02 MPa (1 unit of X & Y axis = 100 m)

4.7. Effect of the Density

The effect of density on the stability of the dump slope structure was evaluated by simulating it from 1300 to 2300 kg/m^3 in the succession of 200 kg/m^3. Figure 4.21 shows that the density had an inverse relationship with the stability of the dump slope structure as the safety factor reduced from 1.49 to 1.36 by increasing the density. The overall reduction in FoS was about 8.72% from 1300 to 2300 kg/m^3. The decrement rate was approximately the same throughout the range. The XDIS and SSI were directly proportional to the density (Figures 4.22 and 4.23). The XDIS increased from 3 to 10 mm, and SSI enhanced from 0.00125 to 0.0035 for the increase in density of the considered range. The XDIS and SSI amplified by 3.34 and 2.8 times, respectively, by varying the density from 1300 to 2300 kg/m^3. The XDIS and SSI increased in each interval, but XDIS was constant between 1700 to 1900 kg/m^3. It was observed that XDIS and SSI were more sensitive toward the stability of the dump slope structure than FoS.

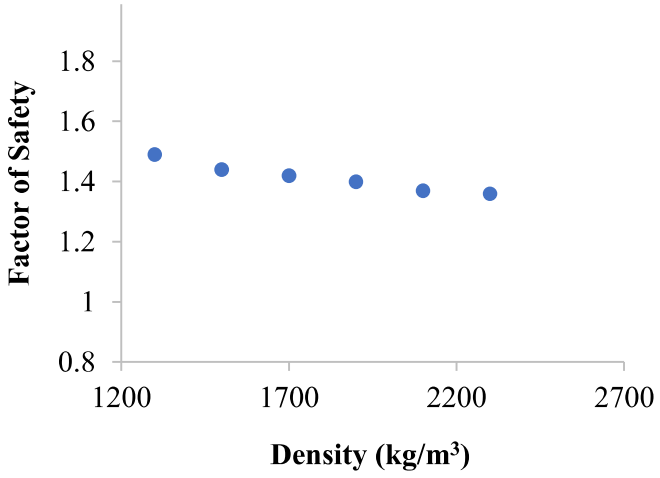

Fig. 4.21 Density versus Factor of Safety

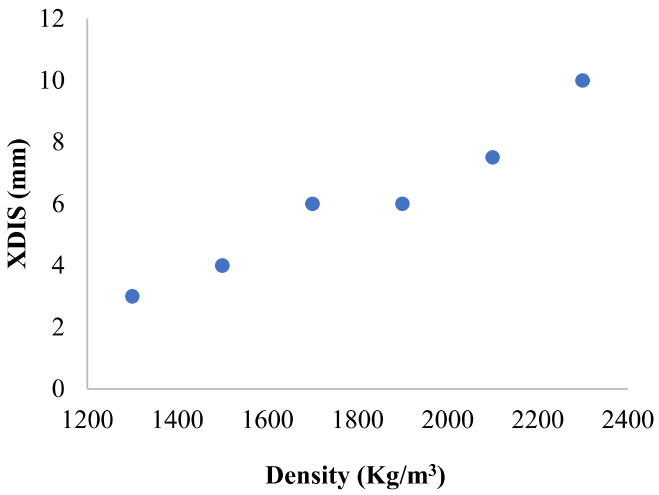

Fig. 4.22 Density versus Max Horizontal Displacement

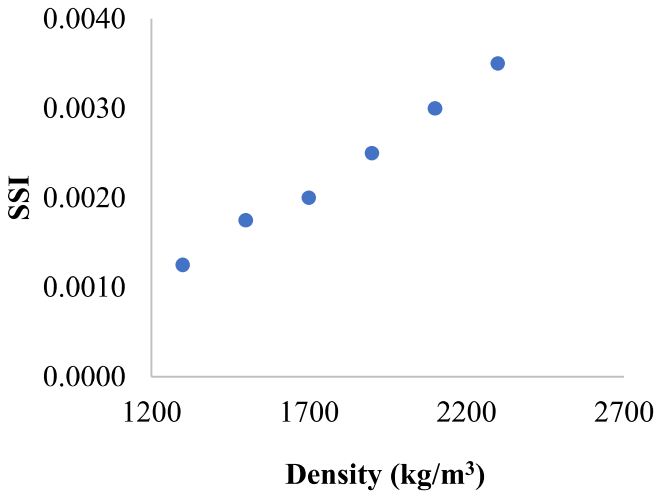

Fig. 4.23 Density versus Max Shear Strain Increment

Figure 4.24 shows the development of the vulnerable zone from the toe of the middle bench when the density was 2300 kg/m^3. The XDIS was very low when the density was less than 2300 kg/m^3.

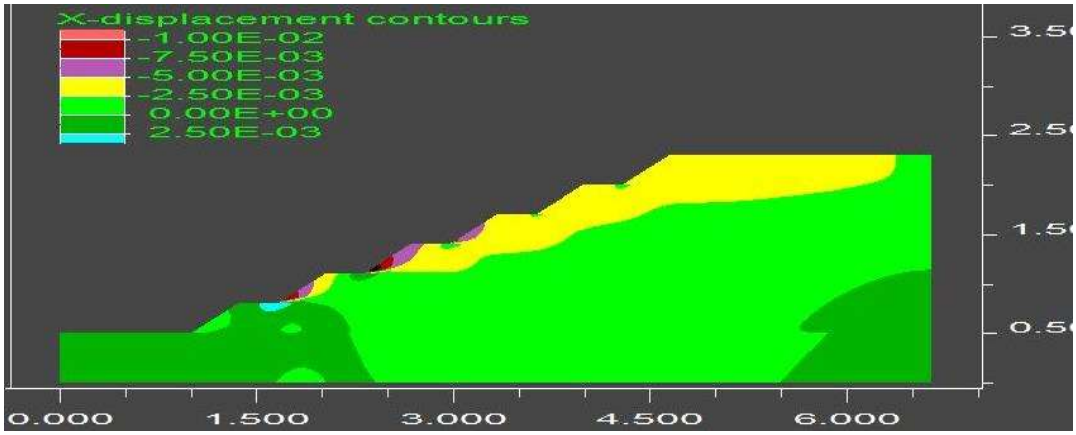

Fig. 4.24 Zone of influence corresponding to density (1 unit of X & Y axis = 100 m)

4.8. Effect of the Friction Angle

The friction angle behaviour was analyzed by increasing it from 16 to 40º. The outcome depicted an almost linear increase in the FoS of the dump slope structure (Figure 4.25). The increase in the friction angle improved the stability of the dump slope structure significantly as the magnitude of the FoS increased from 0.88 to 1.99. The dump slope was unstable at 16º and stabilized at 22º. The max horizontal displacement and shear strain increment subsided sharply from 16 to 22º, and relatively less considerable changes were found with a further increase in the friction angle, as demonstrated in Figures 4.26 (a) and 4.27 (a), respectively. The decrement rate of XDIS and SSI was also notable from 22º to 26º (Figures 4.16 (b) and 4.27 (b)). It was observed that the curve pattern of XDIS and SSI reflected almost identical nature. The XDIS decreased from 80000 to 3 mm, and SSI reduced from 30 to 0.0015 on increasing the friction angle. The SSI was constant between 34 to 40º.

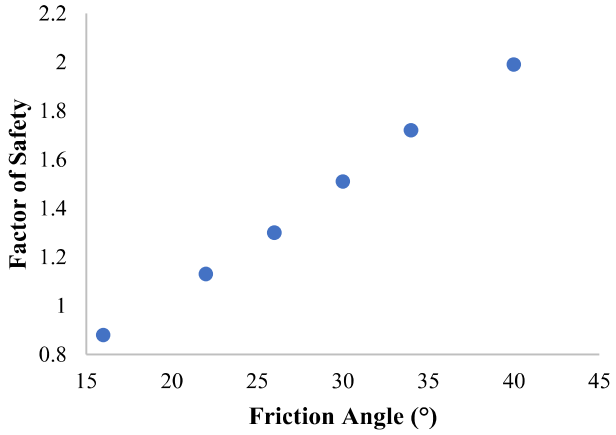

Fig. 4.25 Friction Angle versus Factor of Safety

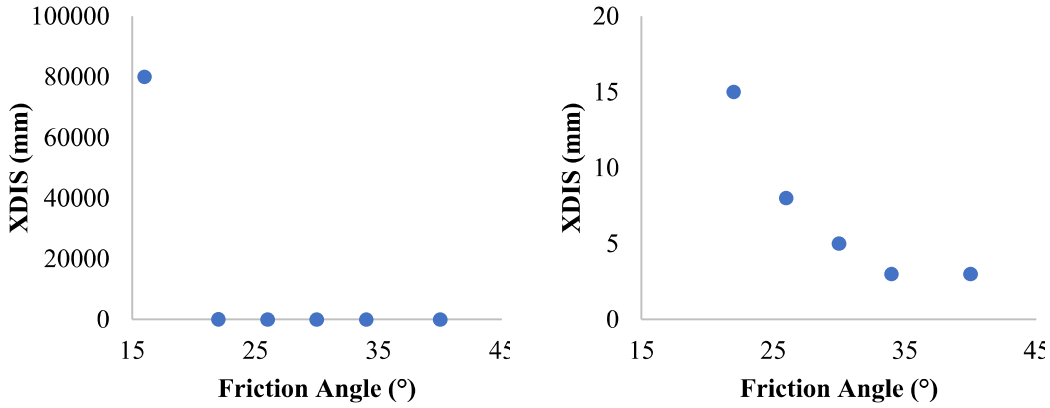

(a) Friction angle 16-40° (b) Friction angle 22-40°

Fig. 4.26 Friction Angle versus Max Horizontal Displacement

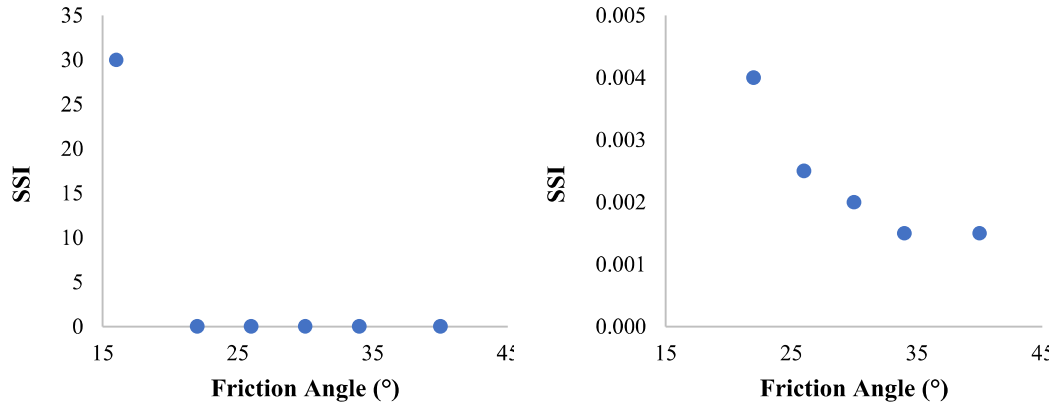

(a) Friction angle 16-40° (b) Friction angle 22-40°

Fig. 4.27 Friction Angle versus Max Shear Strain Increment

The friction angle of the OB dump material was changed in a small interval to understand the increment of the vulnerable zone (Figure 4.28). The vulnerable zone was observed in all benches except the top and bottommost bench at a friction angle of 22° (Figure 4.28 (a)). The extent of the vulnerable zone was higher in the 2nd top most bench. The vulnerable zone increased significantly towards the lower and upper benches upon further reduction in friction angle (Figures 4.28 (b)). The rate of increment of the vulnerable zone was high when dropping the friction angle from 22 to 21°.

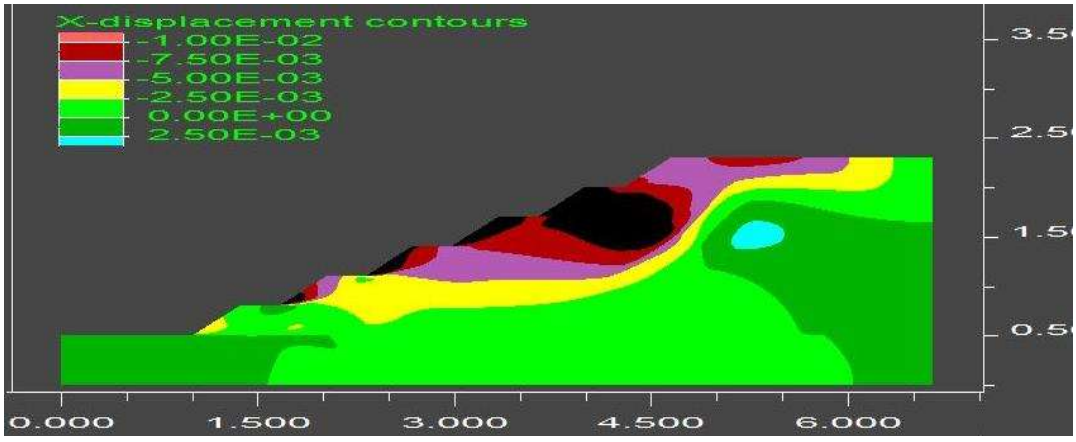

(a) 22°

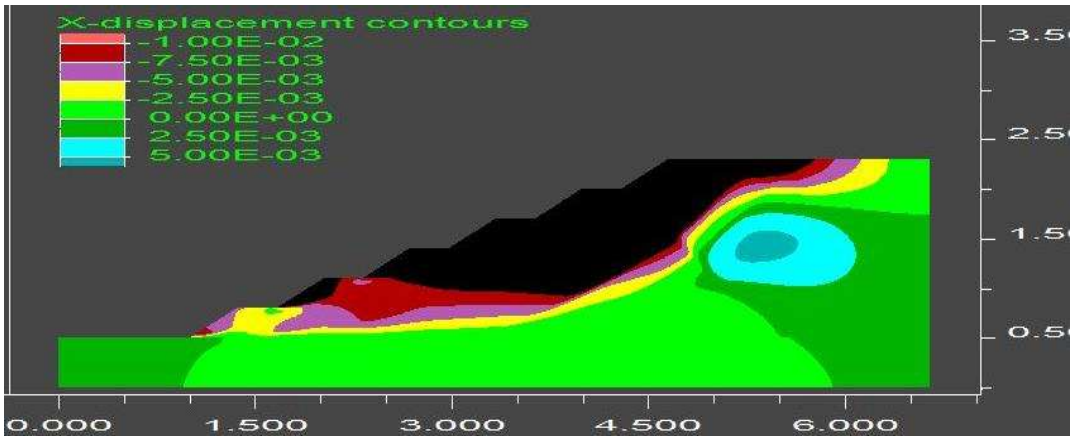

(b) 21°

Fig. 4.28 Zone of influence corresponding to friction angle (1 unit of X & Y axis = 100 m)

4.9. Summary

This chapter described the effect of each stability governing parameter on the stability of the dump slope structure. The parametric study was performed for internal dump slope structures whose base was flat and competent for a predefined range and base values of stability governing parameters.